

Isolation, X-ray Crystal Structure, and Reactivity of a New C–H Carbene Complex of (5,10,15,20-Tetraphenylporphyrinato)ruthenium(II)

Paul Le Maux,[†] Thierry Roisnel,[‡] Irène Nicolas,[†] and Gérard Simonneaux^{*†}

Ingénierie Chimique et Molécules pour le Vivant, and Centre de Diffractométrie, UMR 6226, Université de Rennes 1, Campus de Beaulieu, 35042 Rennes Cedex, France

Received April 1, 2008

The new (porphyrin)ruthenium(II) carbene complex **1** has been prepared by treating (TPP)Ru(CO)(EtOH) with excess 2,6-di-*tert*-butyl-4-methylphenyl diazoacetate and characterized by X-ray crystal structure analysis due to a kinetic stability. The reactivity of **1** toward axial ligands (CO, pyridine, dimethylphenylphosphine) and the asymmetric cyclopropanation of styrene with this bulky diazoacetate ester catalyzed by ruthenium Halterman porphyrin are also presented.

Introduction

The cyclopropanation of olefins using transition metals as catalysts for decomposition of diazo derivatives is one of the best methods to create a carbon–carbon bond in organic synthesis. The most exhaustively studied diazo reagents for intermolecular cyclopropanation reactions are the α -diazoesters, in particular ethyl diazoacetate.^{1–3} Generally, the mechanism of the transition-metal-catalyzed decomposition of α -diazoesters is believed to initially proceed via the formation of a metal carbene complex. Thus several secondary carbene complexes have been prepared and characterized in solution⁴ but very few by X-ray crystallography,⁵ which can be considered as real intermediates directly involved in the catalytic cycle.

Recent growth in the area of transition metal porphyrin chemistry has also been driven by the increased interest associated with ruthenium-catalyzed cyclopropanation. There are two recent reviews on this topic.^{6,7} We⁸ and the groups of Che,⁹ Berkessel,¹⁰ and Gross¹¹ have found many different ruthenium porphyrins that are active catalysts for cyclopropanation of alkenes with diazo derivatives. To date, Che and co-workers^{12,13} have reported the X-ray structures of a wide

variety of porphyrin ruthenium complexes after our first X-ray structure of a ruthenium porphyrin carbene complex in 1998.⁸ Remarkably, all of these structures contain a carbene carbon center bearing two substituents different from hydrogen, due to higher temperature stability. However, these carbene complexes are rarely involved in cyclopropanation reaction. To substantiate the existence of ruthenium carbenes and to more fully characterize the Ru–C bonding, we report herein a combined X-ray crystallographic and reactivity evaluation of the first stable hydrogen carbon ruthenium porphyrin complex. 2,6-Di-*tert*-butyl-4-methylphenyl diazoacetate (DBA), a very bulky diazo ester, previously reported by Doyle,¹⁴ was chosen as diazo derivative due to an expected kinetic stabilization of the resulting ruthenium carbene complex.¹⁵

Results

Synthesis. Reaction of the carbonyl compound (TPP)Ru(CO) with excess of 2,6-di-*tert*-butyl-4-methylphenyl diazoacetate in toluene (70 °C) results in the displacement of the CO ligand after 60 min (Scheme 1). The formation of the brown carbene derivative **1** was observed and, then it was isolated in 91% yield. This carbene is air stable in the solid state and soluble in common polar organic solvents and can be purified by silica gel chromatography. Microcrystals suitable for X-ray structure analysis were obtained by recrystallization from CH₂Cl₂/pentane/THF (1:5:0.01) (vide supra). This new product has been characterized by conventional spectroscopic techniques. In particular, its IR spectrum as a KBr pellet reveals the presence of a single absorption at 1719 cm⁻¹, attributed to the ester group, and the absence of the CO absorption due to the axial ligand.

As indicated by the molecular structure of **1** described below, the carbene complex exists as a six-coordinate, diamagnetic 18-electron species in the solid state. In solution, ¹H NMR studies show that the ligated THF is weakly bound and is in rapid exchange with free THF. For example, broad signals for THF appear at 2.20 and 1.15 ppm at 298 K, whereas at 178 K, these

* Corresponding author. E-mail: gerard.simonneaux@univ-rennes1.fr.

[†] Ingénierie Chimique et Molécules pour le Vivant.

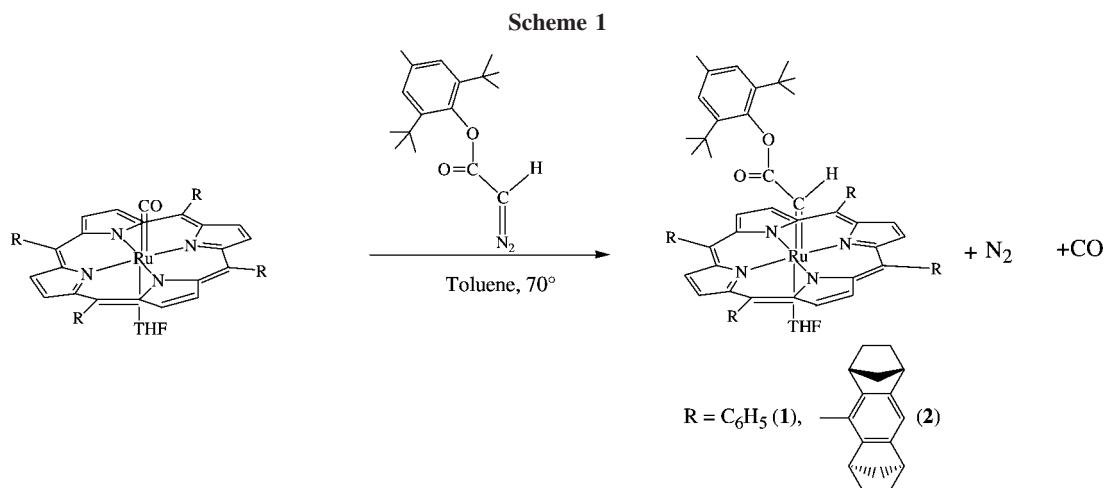
[‡] Centre de Diffractométrie.

- (1) Brookhart, M.; Studabaker, W. B. *Chem. Rev.* **1987**, *87*, 411–432.
- (2) Doyle, M. P.; Forbes, D. C. *Chem. Rev.* **1998**, *98*, 911–935.
- (3) Lebel, H.; Marcoux, J. F.; Molinaro, C.; Charette, A. B. *Chem. Rev.* **2003**, *103*, 977–1050.
- (4) Lee, H. M.; Bianchini, C.; Jia, G.; Barbaro, P. *Organometallics* **1999**, *18*, 1961–1966.
- (5) Werner, H.; Stüer, W.; Wolf, J. R.; Laubender, M.; Weberndörfer, B.; Herbst-Irmer, R.; Lehmann, C. *Eur. J. Inorg. Chem.* **1999**, 1889–1897.
- (6) Simonneaux, G.; Le Maux, P. *Coord. Chem. Rev.* **2002**, *228*, 43–60.
- (7) Che, C. M.; Huang, J. S. *Coord. Chem. Rev.* **2002**, *231*, 151–164.
- (8) Galardon, E.; Le Maux, P.; Toupet, L.; Simonneaux, G. *Organometallics* **1998**, *17*, 565–569.
- (9) Lo, W. C.; Che, C. M.; Cheng, K. F.; Mak, T. C. W. *J. Chem. Soc., Chem. Commun.* **1997**, 1205–1206.
- (10) Frauenkron, M.; Berkessel, A. *Tetrahedron Lett.* **1997**, *38*, 7175–7176.
- (11) Gross, Z.; Galili, N.; Simkhovich, L. *Tetrahedron Lett.* **1999**, *40*, 1571–1574.
- (12) Che, C. M.; Huang, J. S.; Lee, F. W.; Li, Y.; Lai, T. S.; Kwong, H. L.; Teng, P. F.; Lee, W. S.; Lo, W. C.; Peng, S. M.; Zhou, Z. Y. *J. Am. Chem. Soc.* **2001**, *123*, 4119–4129.

(13) Li, Y.; Huang, J. S.; Xu, G. B.; Zu, N.; Zhou, Z. Y.; Che, C. M.; Wong, K. Y. *Chem.–Eur. J.* **2004**, *10*, 3486–3502.

(14) Doyle, M. P.; Bagheri, V.; Wandless, T. J.; Harn, N. K.; Brinker, D. A.; Eagle, C. T.; Loh, K. L. *J. Am. Chem. Soc.* **1990**, *112*, 1906–1912.

(15) Park, S. B.; Sakata, N.; Nishiyama, H. *Chem.–Eur. J.* **1996**, *2*, 303–306.

**Table 1.** ¹H NMR Selected Data for Complexes 1–5^a

complex	porphyrin		carbene ligand			L	
	H _{pyrrole}	H _{H_C=}	H _{Ph}	CH ₃	<i>t</i> -Bu	H _{o,m,p}	CH ₃
1	8.53	14.70	6.59	2.04	0.09	1.15, 2.20	
2	8.42, 8.35	15.18	6.54	2.03	0.07, 0.10		
3	8.16					4.34, 6.55, 6.84	2.33
4	8.15					4.52, 6.49, 6.62	2.14, 2.30
5	7.95					2.37, 5.33, 5.92	

^a L = THF (1), P Me₂Ph (3, 4), pyridine (5).

two resonances appear at -0.2 and -1.1 ppm. Thus, the positions of these signals are strongly shifted upfield relative to those of free THF (3.55 and 1.41 ppm) due to the ring current, this effect being increased at low temperature due to the increased fraction of ligated THF. However, no significant changes of the porphyrin or carbene resonances are observed. The HMQC spectrum shows a typical low-field signal for the carbene carbon at 281.3 ppm. The ¹H NMR spectrum reveals a low-field signal for the hydrogen bound to the carbene carbon at 14.70 ppm (Table 1) and resonances at 6.59 (H Ph), 2.04 (Me), and 0.09 (*t*-Bu) ppm. These three resonances are shifted upfield relative to those of the diazoester, 7.15, 2.35, and 1.4 ppm, respectively, because of the ring current effect. In UV–vis spectroscopy, the coordination of the carbene species slightly modifies the absorption spectrum of the starting carbonyl complex; the Soret band undergoes a 2 nm blue shift when the Q-band becomes broad and appears at 482 nm. All these spectroscopic properties are in agreement with previous data for porphyrin ruthenium carbene complexes.

This method was also found effective for chiral ruthenium porphyrins. Using the Halterman porphyrin,¹⁶ it was possible to isolate the carbene ruthenium porphyrin **2** as a dark brown compound with 93% yield. The ¹H NMR data for **1** and **2** are summarized in Table 1.

Crystal and Molecular Structure of 1. Details of the structure obtained for **1** are given in the Experimental Section.

(16) Halterman, R. L.; Jan, S. T. *J. Org. Chem.* **1991**, *56*, 5253–5254.

(17) Kawai, M.; Yuge, H.; Miyamoto, T. K. *Acta Crystallogr. Sect. C* **2002**, *58*, m581–m582.

(18) Harada, T.; Wada, S.; Yuge, H.; Miyamoto, T. K. *Acta Crystallogr. Sect. C* **2003**, *59*, m37–m39.

(19) Wada, S.; Yuge, H.; Miyamoto, T. K. *Acta Crystallogr. Sect. C* **2003**, *59*, m369–m370.

(20) Scheidt, W. R. Systematics of the Stereochemistry of Porphyrins and Metalloporphyrins. In *The Porphyrin Handbook*; Kadish, K. M., Smith, K. M., Guilard, R., Eds.; Academic Press: San Diego, CA, 2000; Vol. 3, pp 49–112.

Table 2. Crystal Data and Structure Refinement for **1**

empirical formula	C ₆₅ H ₆₀ N ₄ O ₃ Ru
fw	1046.24
temperature	100(2) K
wavelength	0.71073 Å
cryst syst, space group	triclinic, <i>P</i> $\bar{1}$
unit cell dimens	<i>a</i> = 11.0476(16) Å, α = 95.986(8) $^\circ$ <i>b</i> = 11.5485(18) Å, β = 90.096(9) $^\circ$ <i>c</i> = 23.183(4) Å, γ = 116.905(8) $^\circ$
volume	2619.2(7) Å ³
Z, calcd density	2, 1.327 Mg/m ³
absorp coeff	0.351 mm ⁻¹
<i>F</i> (000)	1092
cryst size	0.33 × 0.24 × 0.12 mm
θ range for data collection	3.13 to 27.48 $^\circ$
limiting indices	$-14 \leq h \leq 14$, $-14 \leq k \leq 14$, $-30 \leq l \leq 30$
no. of reflns collected/unique	42 022/11 934 [<i>R</i> (int) = 0.0517]
completeness to $\theta = 27.48$	99.4%
absorp corr	semiempirical from equivalents
max. and min. transmn	0.959 and 0.885
refinement method	full-matrix least-squares on <i>F</i> ²
no. of data/restraints/params	11 934/0/666
goodness-of-fit on <i>F</i> ²	1.255
final <i>R</i> indices [<i>I</i> > 2 σ (<i>I</i>)]	<i>R</i> 1 = 0.0666, w <i>R</i> 2 = 0.1287
<i>R</i> indices (all data)	<i>R</i> 1 = 0.0728, w <i>R</i> 2 = 0.1311
largest diff peak and hole	2.285 and -2.011 e Å ⁻³

Table 3. Selected Bond Distances (Å) and Angles (deg) for **1**

Ru(1)–C(31)	1.839(4)	Ru(1)–N(4)	2.054(3)
Ru(1)–N(1)	2.042(3)	Ru(1)–O(51)	2.376(3)
Ru(1)–N(2)	2.053(3)	C(31)–C(32)	1.480(5)
Ru(1)–N(3)	2.057(3)	C(31)–H(31)	0.9500
C(31)–Ru(1)–N(1)	94.40(14)	N(3)–Ru(1)–O(51)	88.43(10)
C(31)–Ru(1)–N(2)	96.39(14)	N(4)–Ru(1)–O(51)	85.47(10)
C(31)–Ru(1)–N(3)	92.52(14)	N(1)–Ru(1)–N(3)	173.08(12)
C(31)–Ru(1)–N(4)	90.02(14)	N(2)–Ru(1)–N(4)	173.58(12)
C(31)–Ru(1)–O(51)	175.38(13)	C(32)–C(31)–Ru(1)	127.6(3)
N(1)–Ru(1)–O(51)	84.69(11)	C(32)–C(31)–H(31)	116.2
N(2)–Ru(1)–O(51)	88.13(10)	Ru(1)–C(31)–H(31)	116.2

Table 2 lists crystallographic data for **1**; selected bond distances and bond angles are given in Table 3. The carbene complex **1** forms as dark brown crystals in the triclinic space group *P* $\bar{1}$ with two molecules per unit cell. Figure 1 illustrates the molecular structure and atom labeling. As indicated in the structure, the carbene complex exists as a six-coordinate compound, with a THF molecule as axial ligand. As expected for such a complex, the porphyrin ligand is nearly planar. However, the ruthenium atom is slightly out of the mean plane of the porphyrin plane, 0.10 Å toward the carbene ligand. A similar situation has been previously observed with other

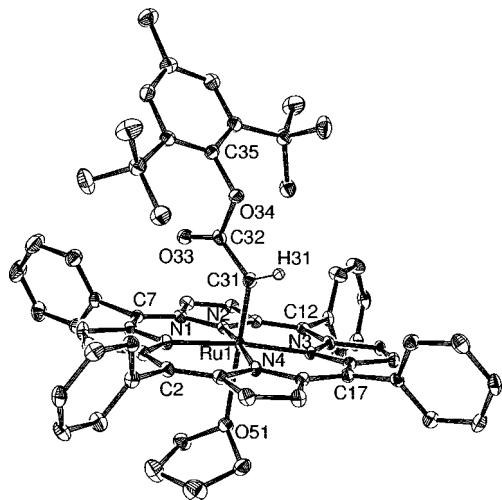


Figure 1. ORTEP drawing and atom labeling of **1**.

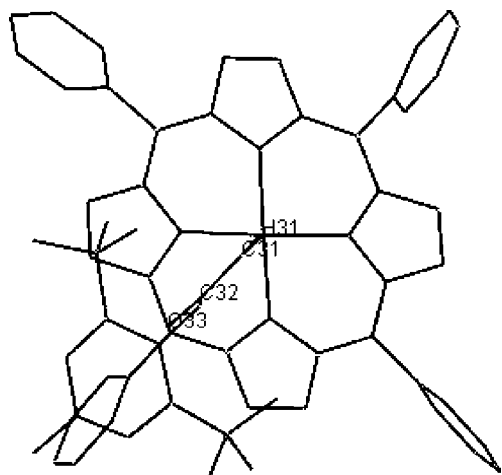


Figure 2. Figure showing the dihedral angle φ (between the plane of the ligand and the plane defined by a porphyrinato nitrogen atom, the metal, and the carbene ligand carbon atom).

porphyrin ruthenium complexes.⁸ The Ru–N distances of 2.042(3)–2.054(3) Å all fall within the range previously reported for diamagnetic ruthenium porphyrin complexes.^{8,13,17–19} The geometry of the coordination sphere is close to an octahedral geometry. Bond angles at ruthenium are in the range 90.02(14)–96.39(14)° for *cis* angles and 173.08(12)–173.58(12)° for *trans* angles. The O–Ru–C(carbene) angle is 175.38(13)°. Such values, which are significantly different from expected values for an ideal octahedral geometry, are probably related to steric interactions between the bulky ester group and the phenyl groups of the porphyrin. The carbene fragment is distorted, since the angle formed by C(32)–C(31)–H(31) is 116.2°, a value that is significantly smaller than 120°, the angle expected for ideal sp² hybridization.

The stereochemical constraints that result from the steric interaction of the axial ligand atoms with atoms of the porphyrinato core have recently been discussed in a review reported by Scheidt.²⁰ The orientation of the ligand can be specified by the dihedral angle φ between the plane of the ligand and a plane defined by a porphyrinato nitrogen atom, the metal atom (Ru), and the ligand carbon (carbene) atom. Minimum steric interaction will occur for a dihedral angle of 45°. For complex **1**, this angle is 45.15° (Figure 2), showing the importance of the steric interaction due to the large ester group. In addition, the phenyl of the carbene ligand has its plane

perpendicular to the plane formed by Ru(1)–C(31)–C(32)–H(31). This presumably decreases the intramolecular strain of the two *tert*-butyl groups pointing toward the porphyrin ring. Thus the orientation of the phenyl ring of the ester group is such that it renders difficult the nucleophilic attack of any substrate onto the electrophilic carbene center. This situation explains the kinetic stabilization of complex **1**.

The Ru–C distance of 1.839(4) Å is slightly longer than the ruthenium–carbon double bond (1.829(9) Å) for (TPP)Ru–[C(CO₂Et)](MeOH) reported by us⁸ some years ago and similar to those reported by Che¹³ and Miyamoto.^{13,17–19} The Ru–O (THF) distance 2.376(3) Å is shorter than the axial Os–O bond (THF, 2.43(2) Å) in a similar carbene osmium complex, reported by Woo et al.,²¹ as expected from the different size of the two metal atoms.

Ligand-Exchange Reactions. We decided to investigate the reaction of **1** and **2** with stronger σ -donor ligands, such as dimethylphenylphosphine. The titration curve is shown in Figure 3. Modification of the wavelength of the Soret band reveals the presence of an intermediate (λ_{max} 412 nm) that appears after addition of 1 equiv of ligand. This intermediate is probably the mixed phosphine-carbene complex.⁸ Addition of a large excess of phosphine results in the formation of the symmetric bis-ligated derivative, as identified by UV–vis and ¹H NMR (Table 1).

We also investigated the interaction of **1** and CO. During slow bubbling of carbon monoxide in a solution of toluene, the carbene ligand is completely displaced after 8 h at 100 °C. Thus the reaction mixture progressively turns red and a precipitate appears, which is easily characterized by IR and NMR as a mixture of (TPP)Ru(CO) and (TPP)Ru(CO)₂.²²

Treatment of **1** with excess of pyridine did not allow isolation of the corresponding six-coordinate ruthenium porphyrin carbene complex. For example, addition of an excess of pyridine to a solution of **1** in dichloromethane afforded (TPP)Ru(Pyr)₂, which was isolated in 78% yield. This contrast with the reactivity of the ruthenium porphyrin bis-phenyl carbene complex toward pyridine; in this case the mixed ligated complex was obtained.¹³

Catalytic Carbene Transfer Reactions. To determine if the increase of the bulkiness of the diazo derivative occurs with changes in reactivity, catalytic experiments were first performed without olefins to obtain formerly the dimerization of the carbenes. In contrast to results obtained with ethyl diazoacetate leading mainly to maleate, no dimerization was observed in the presence of a catalytic amount of (TPP)Ru(CO) at 100 °C.

Then, we examined the possibility of the bulky carbene transfer reaction to styrene, although the carbene complex is quite stable. The addition of 2,6-di-*tert*-butyl-4-methylphenyl diazoacetate to styrene catalyzed by TPPRuCO was carried out to give in 70% yield the corresponding 2-phenylcyclopropane-1-carboxylate with pure *trans* geometry (Scheme 2, Table 4). The reaction conditions were quite drastic since it was necessary to heat at 100 °C for 12 h.

The asymmetric version was also tested using Halterman porphyrin as chiral ligand (Schemes 1 and 2). To evaluate the reactivity of the bulky diazoacetate, its ruthenium-catalyzed decomposition was examined in the presence of styrene in toluene at 65 °C by using **2** as catalyst (Table 4). The diazo derivatives were added slowly to the reaction mixture over 1 h, and the reaction was stopped after 12 h. The cyclopropane was

(21) Djukic, J. P.; Smith, D. A.; Young, V. G.; Woo, L. K. *Organometallics* **1994**, *13*, 3020–3026.

(22) Eaton, G. R.; Eaton, S. S. *J. Am. Chem. Soc.* **1975**, *97*, 235–236.

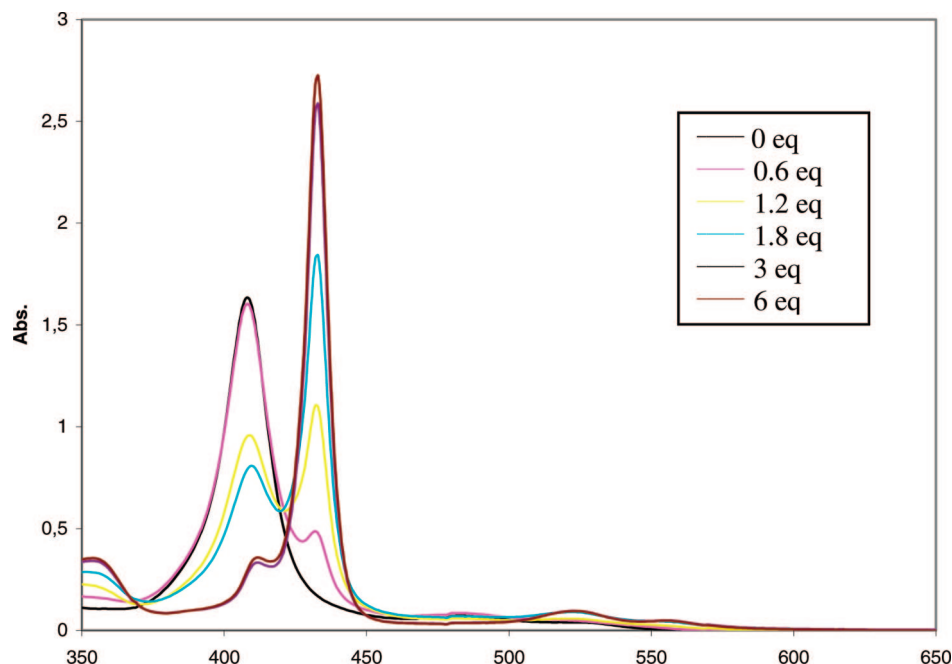


Figure 3. UV-vis titration curves of a solution of **1** in CH_2Cl_2 (10 mg, 10.2 μM) with PMe_2Ph .

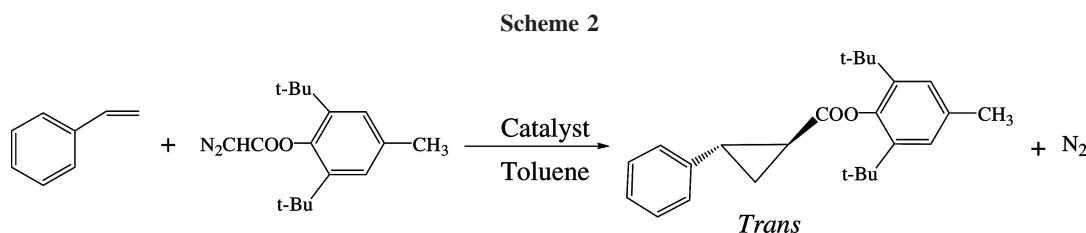


Table 4. Cyclopropanation of Styrene with 2,6-Di-*tert*-butyl-4-methylphenyl Diazoacetate Catalyzed by Ru Porphyrins **1** and **2**^a

catalyst	temperature (°C)	yield ^b (%)	<i>trans</i> (%)	<i>ee</i> _{<i>trans</i>} ^c (%)
1	100	70	100	
2	65	62	100	60

^a Reactions were performed in toluene for 12 h with a catalyst: diazo:substrate molar ratio of 1:200:1000. ^b Yields were based on isolated cyclopropane. ^c Determined by chiral HPLC using a Chiralcel OD column.

formed with 62% yield and 60% enantioselectivity for the *trans* isomer (Table 4). The formation of the *cis* isomer was not detected.

Then, we investigated the potential of **1** as a catalyst for the cyclopropanation of styrene by EDA. The diazo derivatives were added slowly to the reaction mixture over 1 h, and the reaction was stopped after 12 h. The cyclopropane was formed with 95% yield and 13:1 *trans*:*cis* ratio.

Discussion

The use of metalloporphyrins as cyclopropanation catalysts has been proposed by Callot et al., who first reported that rhodium porphyrins provided a *cis* preference for the cyclopropanation of styrene with ethyl diazoacetate.²³ Since then, numerous examples involving rhodium,^{24,25} osmium,^{26,27} co-

balt,²⁸ and iron^{29–32} porphyrins as catalysts have been reported. Rhodium catalysts produce synthetically useful excesses of *cis* cyclopropyl esters using ethyl diazoacetate as the carbene source, whereas, in the same conditions, osmium and iron catalysts mainly provide the *trans* product. Despite the relationship between ruthenium, iron, and osmium and the synthesis of different carbene complexes of ruthenium porphyrins, nicely developed by Collman et al.,³³ it is more recently that cyclopropanation^{9,10,34} and ethyl diazoacetate insertion into heteroatom bond reactions³⁵ were observed using ruthenium porphyrins as catalysts. This renewal of interest in reactions catalyzed by ruthenium(II) porphyrin complexes is related to the simultaneous development of new chiral ruthenium porphyrins. However, the preparation of transition metal carbene complexes that lack direct heteroatom stabilization of the

(26) Smith, D. A.; Reynolds, D. N.; Woo, L. K. *J. Am. Chem. Soc.* **1993**, *115*, 2511–2513.

(27) Hamaker, C. G.; Djukic, J. P.; Smith, D. A.; Woo, L. K. *Organometallics* **2001**, *20*, 5189–5199.

(28) Huang, L.; Chen, Y.; Gao, G. Y.; Zhang, X. P. *J. Org. Chem.* **2003**, *68*, 8179–8184.

(29) Wolf, J. R.; Hamaker, C. G.; Djukic, J. P.; Kodadek, T.; Woo, L. K. *J. Am. Chem. Soc.* **1995**, *117*, 9194–9199.

(30) Hamaker, C. G.; Mirafzal, G. A.; Woo, L. K. *Organometallics* **2001**, *20*, 5171–5176.

(31) Li, Y.; Huang, J. S.; Zhou, Z. Y.; Che, C. M.; You, X. Z. *J. Am. Chem. Soc.* **2002**, *124*, 13185–13193.

(32) Tagliatesta, P.; Pastorini, A. *J. Mol. Catal. A: Chem.* **2003**, *198*, 57–61.

(33) Collman, J. P.; Brothers, P. J.; McElwee-White, L.; Rose, E.; Wright, L. J. *J. Am. Chem. Soc.* **1985**, *107*, 4570–4571.

(34) Galardon, E.; Le Maux, P.; Simonneaux, G. *J. Chem. Soc., Chem. Commun.* **1997**, 927–928.

(35) Galardon, E.; Le Maux, P.; Simonneaux, G. *J. Chem. Soc., Perkin Trans. 1* **1997**, 2455–2456.

(23) Callot, H. J.; Piechocki, C. *Tetrahedron Lett.* **1980**, *21*, 3489–3492.

(24) Maxwell, J. L.; Brown, K. C.; Bartley, D. W.; Kodadek, T. *Science* **1992**, *256*, 1544–1547.

(25) Maxwell, J. L.; O'Malley, S.; Brown, K. C.; Kodadek, T. *Organometallics* **1992**, *11*, 645–652.

electrophilic carbene carbon center is still of interest owing to the high reactivity of these species in comparison with that of heteroatom-stabilized systems and the relevance of these complexed divalent species as possible intermediates in the catalytic mechanism.

The stability of the carbene complex **1** is in marked contrast with its congener resulting from reaction of (TPP)Ru(CO) with ethyl diazoacetate, which is stable only at very low temperature ($-70\text{ }^{\circ}\text{C}$). This important increase in thermal stability is associated with a large steric effect of the ester substituent. Thus the most interesting feature of the structure of complex **1** is the steric congestion due to the presence of the bulky ester group on the carbene ligand. An interesting structural feature is the orientation of the carbene ligand, the value of the carbene–porphyrin dihedral angle being ($\varphi = 45.15^{\circ}$) (Figure 2). Importantly, the steric constraints also appear to limit access to the electrophilic carbene center and prevent substrate approach. The two *tert*-butyl groups and the phenyl group of the carbene ligand seem to form a “cap” above the plane of the porphyrin ring and protect the carbene center from reacting species. As a second consequence of the bulkiness of the diazo ester compound, higher temperatures are needed for the cyclopropanation reaction, which gave the *trans* isomer as the sole product. A similar conclusion was also obtained using the same diazo derivatives but with two different catalytic systems.^{14,15} As expected, no dimerization of the carbene was observed.

In conclusion, we have substantiated the mechanism of the asymmetric cyclopropanation of olefins with diazoacetates catalyzed by ruthenium porphyrins by isolation and X-ray structure determination of the corresponding carbene complexes as active intermediates.

Experimental Section

General Experiments. All reactions were performed under argon and were magnetically stirred. Solvents were distilled from appropriate drying agent prior to use: toluene from sodium and benzophenone, CH_2Cl_2 from CaH_2 , CHCl_3 from P_2O_5 . Commercially available reagents were used without further purification unless otherwise stated. All reactions were monitored by TLC with Merck precoated aluminum foil sheets (silica gel 60 with fluorescent indicator UV₂₅₄). Compounds were visualized with UV light at 254 and 365 nm. Column chromatographies were carried out using silica gel from Merck (0.063–0.200 mm). ^1H NMR and ^{13}C NMR in CDCl_3 were recorded using Bruker (Advance 500dpx and 300dpx) spectrometers at 500 and 75 MHz, respectively. UV–visible spectra were recorded on a UVIKON XL from Biotec. Infrared spectra were performed in KBr disks in a IFS 28 Bruker. The enantiomeric excess of the cyclopropane was determined on a Varian Prostar 218 system equipped with a Chiralcel OD-H column.

The porphyrins were synthesized by literature methods: *meso*-tetrakis-5,10,15,20-phenylporphyrin (TPPH₂) and [(1*S*,4*R*,5*R*,8*S*)-1,2,3,4,5,6,7,8-octahydro-1,4:5,8-dimethanoanthracene-9-yl]porphyrin (HaltH₂).¹⁶ The corresponding ruthenium carbonyl complexes, (TPP)Ru(CO) and (Halt)Ru(CO), were obtained by refluxing the porphyrins in *o*-dichlorobenzene with $\text{Ru}_3\text{CO}_{12}$ at $180\text{ }^{\circ}\text{C}$.⁶ The 2,6-di-*tert*-butyl-4-methylphenyl diazoacetate was obtained according to the procedure of Doyle.¹⁴ Methanesulfonyl azide was prepared from methanesulfonyl chloride and sodium azide.

Synthesis of (TPP)Ru [:(CH(CO₂-2,6-di-*tert*-butyl-4-methylphenyl)](THF), **1.** A solution of 2,6-di-*tert*-butyl-4-methylphenyl diazoacetate (58 mg (0.202 mmol) in 5 mL of dry toluene) was added to a solution of (TPP)Ru(CO) (100 mg, 0.134 mmol) in 30 mL of dry toluene at $70\text{ }^{\circ}\text{C}$ under argon. The reaction was monitored by thin-layer chromatography, and after 1 h, the solvent was removed under vacuum. The crude product was purified by silica

gel column chromatography under argon (CH_2Cl_2 /pentane, 1:4) to give 120 mg of a dark brown product (91%). Microcrystals suitable for X-ray structure analysis were obtained by recrystallization from CH_2Cl_2 /pentane/THF (1:5:0.01). ^1H NMR (CDCl_3 , ppm): δ 8.53 (s, 8H); 8.12 (m, 8H); 7.73 (m, 12H); 6.59 (s, 2H); 2.04 (s, 3H); 0.09 (s, 18H). HMQC: ^1H , 14.70 (s, HC=); ^{13}C , 281.30 (HC=). UV–vis (CH_2Cl_2) λ_{max} /nm (log ϵ): 408 (5.22); 482 (3.98). IR (KBr, cm^{-1}): 1719. HRMS: calcd for $\text{C}_{61}\text{H}_{53}\text{N}_4\text{O}_2\text{Ru}$ 975.3212 ($\text{M} + \text{H}^+$), found 975.3230.

Synthesis of (Halt)Ru[:(CH(CO₂-2,6-di-*tert*-butyl-4-methylphenyl)](THF), **2.** A solution of 2,6-di-*tert*-butyl-4-methylphenyl diazoacetate (34 mg, 0.117 mmol, in 5 mL of dry toluene) was added to a solution of (Halt)Ru(CO) (100 mg, 0.078 mmol) in 30 mL of dry toluene at $70\text{ }^{\circ}\text{C}$ under argon. The reaction was monitored by thin-layer chromatography, and after 30 min, the solvent was removed under vacuum. The crude product was purified by a silica gel column under argon (CH_2Cl_2 /pentane, 1:4) to give 110 mg of a dark brown product (93%). ^1H NMR (CDCl_3 , ppm): 8.42 (d, 4H, $J = 4.8$ Hz); 8.35 (d, 4H, $J = 4.8$ Hz); 7.36 (s, 4H); 6.54 (s, 2H); 3.60 (d, 4H, $J = 2.4$ Hz); 3.53 (d, 4H, $J = 2.7$ Hz); 3.10 (d, 4H, $J = 2.8$ Hz); 2.41 (d, 4H, $J = 2.8$ Hz); 2.03 (s, 3H); 1.89–2.02 (m, 16H); 1.22–1.49 (m, 24H); 0.92 (t, 8H, $J = 7.0$ Hz); 0.10 (s, 9H); 0.07 (s, 9H). HMQC: ^1H , 15.18 (s, HC=); ^{13}C , 278.39 (C=). UV–vis (CH_2Cl_2): λ_{max} /nm (log ϵ) 409 (5.15); 480 (3.58). IR (KBr, cm^{-1}): 1723. HRMS: calcd for $\text{C}_{101}\text{H}_{101}\text{N}_4\text{O}_2\text{Ru}$ 1503.6968 ($\text{M} + \text{H}^+$), found 1503.6992.

Ligand-Exchange Reaction of **1 with PMe_2Ph . Synthesis of (TPP)Ru(PMe_2Ph)₂, **3**.** To a solution of **1** (10 mg, 10.2 μmol) in 1 mL of CH_2Cl_2 was added via syringe 6 equiv of PMe_2Ph . The titration was monitored by UV–vis spectroscopy (Figure 3). The bis-phosphine complex **3** was purified by silica gel column chromatography (CH_2Cl_2 /pentane, 1:4) to give 9 mg of a red-brown product (90%). ^1H NMR (CDCl_3 , ppm): δ 8.16 (s, 8H); 7.94–7.98 (m, 8H); 7.65–7.71 (m, 12H); 6.84 (t, 2H, $J = 6$ Hz); 6.55 (t, 4H, $J = 6$ Hz); 4.29–4.38 (m, 4H); 2.33 (t, 6H, $J = 4$ Hz). ^{31}P NMR (CDCl_3 , ppm): 2.12. UV–vis (CH_2Cl_2): λ_{max} /nm (log ϵ) 433 (5.12); 522 (4.01).

Ligand-Exchange Reaction of **2 with PMe_2Ph . Synthesis of (Halt)Ru(PMe_2Ph)₂, **4**.** To a solution of **2** (90 mg, 60 μmol) in 1 mL of CH_2Cl_2 was added via syringe 2.5 equiv of PMe_2Ph . The reaction was monitored by UV–vis spectroscopy and TLC. The bis-phosphine complex **4** was purified by silica gel column chromatography (CH_2Cl_2 /pentane, 1:4) to give 80 mg of a red-brown product (89%). ^1H NMR (CDCl_3 , ppm): δ 8.15 (s, 8H); 7.30 (s, 4H); 6.62 (t, 2H); 6.49 (t, 4H); 4.52 (m, 4H); 3.54 (s, 8H); 2.63 (s, 8H); 1.83–1.99 (m, 16H); 1.31–1.43 (m, 24H); 0.89–0.96 (m, 8H); 2.14 (s, 6H); 2.30 (s, 6H). ^{31}P NMR (CDCl_3 , ppm): -3.03 . UV–vis (CH_2Cl_2): λ_{max} /nm (log ϵ) 433 (5.34); 524 (3.94).

Ligand-Exchange Reaction of **1 with Pyridine. Synthesis of (TPP)Ru(pyridine)₂, **5**.** To a solution of **1** (10 mg, 10.2 μmol) in 1 mL of CH_2Cl_2 was added via syringe 100 equiv of pyridine. The titration was monitored by UV–vis spectroscopy. The bis-pyridine complex **5** was purified by silica gel column chromatography (CH_2Cl_2 /pentane, 1:4) to give 7 mg of a yellow-brown product (78%). ^1H NMR (CDCl_3 , ppm): δ 7.95 (s, 8H); 7.67, 7.58 (2m, 20H); 5.92 (t, 2H, $J = 6.2$ Hz); 5.33 (t, 4H, $J = 6.4$ Hz); 2.37 (d, 4H, $J = 5.2$ Hz). UV–vis (CH_2Cl_2): λ_{max} /nm (log ϵ) 409 (5.13); 505 (4.42).

Ligand-Exchange Reaction of **1 with CO.** Carbon monoxide was bubbled through a solution of 10 mg (10.2 μmol) of **1** in 1 mL of toluene at $100\text{ }^{\circ}\text{C}$ for 8 h. A red precipitate appeared, and after isolation the product was identified by its IR spectrum as a mixture of (TPP)Ru(CO) and (TPP)Ru(CO)₂, 1953 and 2015 cm^{-1} , respectively, as previously reported.²²

Catalytic Cyclopropanation of Styrene by Catalyst **1.** The diazo compound 2,6-di-*tert*-butyl-4-methylphenyl diazoacetate (57.6 mg, 0.2 mmol) dissolved in 0.2 mL of toluene was added at a

controlled rate over a 1 h period to a stirred solution of 104 mg (1 mmol) of styrene and 0.74 mg (1 μ mol) of the catalytic precursor (TPP) Ru CO in 1 mL of toluene at 100 °C. After it was stirred at 100 °C for 12 h, the reaction solution was passed through a short silica gel column (pentane/CH₂Cl₂, 4:1) to remove the catalyst and excess styrene. After evaporation of solvents, the cyclopropane product (45 mg, 70%) was characterized by ¹H NMR as *trans*-2,6-di-*tert*-butyl-4-methylphenyl-2-phenylcyclopropane-1-carboxylate. ¹H NMR (CDCl₃, ppm): 7.22–7.45 (m, 5H); 7.17 (s, 2H); 2.70–2.80 (m, 1H); 2.37 (s, 3H); 2.18–2.28 (m, 1H); 1.53–1.63 (m, 1H); 1.41 (s, 9H); 1.40 (s, 9H).

Catalytic Cyclopropanation of Styrene by Catalyst 2. The diazo compound 2,6-di-*tert*-butyl-4-methylphenyl diazoacetate (57.6 mg, 0.2 mmol) dissolved in 0.2 mL of toluene was added at a controlled rate over a 1 h period to a stirred solution of 104 mg (1 mmol) of styrene and 1.2 mg (1 μ mol) of the catalytic precursor (Halt) Ru CO in 1 mL of toluene at 65 °C. After it was stirred at 65 °C for 12 h, the reaction solution was passed through a short silica gel column (pentane/CH₂Cl₂, 4:1) to remove the catalyst and excess styrene. After evaporation of solvents, the cyclopropane product (45 mg, 62%) was characterized by ¹H NMR as *trans*-2,6-di-*tert*-butyl-4-methylphenyl-2-phenylcyclopropane-1-carboxylate. The ee (=60%) was determined by chiral HPLC using a Chiralcel OD column, *n*-hexane/*i*PrOH = 99:1, flow rate = 0.2 mL/min, wavelength = 220 nm, *t*_R = 13.96 min for the minor isomer, *t*_R = 15.98 min for the major isomer. $[\alpha]_D^{23} = +120$ (CH₂Cl₂).

(36) Altomare, A.; Burla, M. C.; Camalli, M.; Cascarano, G.; Giacovazzo, C.; Guagliardi, A.; Moliterni, A. G.; Polidori, G.; Spagna, R. *J. Appl. Crystallogr.* **1999**, 32, 115–119.

Catalytic Cyclopropanation of Styrene by Catalyst 1 with Ethyl Diazoacetate. The ethyl diazoacetate (22.8 mg, 0.2 mmol) dissolved in 0.2 mL of toluene was added at a controlled rate over a 1 h period to a stirred solution of 104 mg (1 mmol) of styrene and 0.97 mg (1 μ mol) of the catalyst **1** in 1 mL of toluene at ambient temperature. After it was stirred for 12 h, the reaction solution was analyzed by GC (95%, *trans/cis* 13:1).

X-ray Crystallographic Structure Determination of 1. Intensity data were collected on a Bruker-AXS diffractometer at *T* = 100(2) K. The structure was solved by direct methods using the SIR97 program³⁶ and then refined with full-matrix least-squares methods based on *F*² (SHELX-97)³⁷ with the aid of the WINGX program.³⁸ All non-hydrogen atoms were refined with anisotropic thermal parameters. H atoms were finally included in their calculated positions. A final refinement on *F*² with 11 934 unique intensities and 666 parameters converged at $\sigma R(F^2) = 0.1287$ (*R*(*F*) = 0.0666) for 11 199 observed reflections with *I* > 2 σ (*I*).

Supporting Information Available: Tables of atomic coordinates, bond lengths and angles, anisotropic displacement parameters, and torsional angles. This material is available free of charge via the Internet at <http://pubs.acs.org>.

OM800289V

(37) Sheldrick, G. M. *SHELX97, Programs for Crystal Structure Analysis (Release 97-2)*; Institut für Anorganische Chemie der Universität: Göttingen, Germany, 1998.

(38) Farrugia, L. J. *J. Appl. Crystallogr.* **1999**, 32, 837–838.